Nucleic Acids Research, 1998, Vol. 26, No. 23 **5441–5447**

Dehydromonocrotaline generates sequence-selective N-7 guanine alkylation and heat and alkali stable multiple fragment DNA crosslinks

Tamara N. Pereira[1,2], Richard I. Webb[3], Paul E. B. Reilly[2], Alan A. Seawright[1] and Arungundrum S. Prakash[1,*]

[1]National Research Centre for Environmental Toxicology, 39 Kessels Road, Coopers Plains, QLD 4108, Australia and [2]Department of Biochemistry and [3]Centre for Microscopy and Microanalysis, The University of Queensland, St Lucia, QLD 4072, Australia

Received July 27, 1998; Revised and Accepted October 15, 1998

ABSTRACT

Monocrotaline is a pyrrolizidine alkaloid known to cause toxicity in humans and animals. Its mechanism of biological action is still unclear although DNA crosslinking has been suggested to a play a role in its activity. In this study we found that an active metabolite of monocrotaline, dehydromonocrotaline (DHM), alkylates guanines at the N7 position of DNA with a preference for 5′-GG and 5′-GA sequences. In addition, it generates piperidine- and heat-resistant multiple DNA crosslinks, as confirmed by electrophoresis and electron microscopy. On the basis of these findings, we propose that DHM undergoes rapid polymerization to a structure which is able to crosslink several fragments of DNA.

INTRODUCTION

Pyrrolizidine alkaloids (PAs) are a group of toxins which are present in plants of widespread geographical distribution. They have been recognized as being of human and veterinary concern since the turn of the century and have resulted in several episodes of fatal poisoning in humans (1–5) as well as livestock (6–9). The acute toxic syndrome is characterized by hepatic veno-occlusive disease, pulmonary hypertension and right ventricular hypertrophy. Long-term ingestion of PAs results in liver fibrosis progressing to cirrhosis and is typified by the presence of abnormally large hepatocytes, termed megalocytes. The chronic disease is poorly understood. Although megalocytosis is believed to be due to the antimitotic action of the alkaloids, studies have also demonstrated the carcinogenicity of these compounds upon chronic administration to rodents (10–14).

The parent alkaloids are not toxic but are metabolized by hepatic cytochrome P450 enzymes (15) to pyrroles (Fig. 1) The highly electrophilic nature of these pyrroles ensures that they react readily with nucleophilic tissue constituents such as DNA (16,17) and proteins (18). Some pyrroles, such as dehydromonocrotaline (DHM), have two electrophilic sites. Such bifunctional pyrroles can alkylate DNA and subsequently form interstrand DNA–DNA (19,20) as well as DNA–protein crosslinks (21). Alkylation at one position alone is sufficient for toxicity, as shown by the cytotoxic effect of the synthetic monofunctional pyrrole, 3-hydroxy methyl-1,2-dimethyl pyrrole, in cell culture (22). However, a correlation does exist between the cytotoxicity and crosslinking abilities of PAs (19).

The exact nature of the DNA–pyrrole interaction is not well characterized. Robertson (16) showed that dehydroretronecine (DHR), a bifunctional metabolite of the PA monocrotaline (Fig. 1), binds to nucleophiles via the C7 and C9 positions, a reaction that does not involve the pyrrole ring. In this study, DHR was shown to bind to the exocyclic amino group (N2) of deoxyguanosine. However, its reactivity with double-stranded DNA may be different. It is pertinent to note that the antitumor antibiotic mitomycin C, a close analog of DHM, has been shown to alkylate at N7 guanines in the major groove (23) and form interstrand crosslinks via N2 guanine in the minor groove (23,24). The protein–pyrrole interaction is less well characterized. Robertson *et al.* (18) have shown that pyrroles bind via the C7 position to the sulfhydryl groups of cysteine and glutathione. Seawright *et al.* (25) demonstrated a similar interaction with the sulphydryl group of haemoglobin. These studies suggest that the pyrroles are likely to bind to other proteins involved in the regulation of the cell.

In addition to the alkylation of cellular nucleophiles, the pyrrole itself has a nucleophilic centre at the double bond of C2 and C3. Thus, pyrrolic esters (and to a lesser extent pyrrolic alcohols) polymerize readily *in vitro* via acid catalysis (26). It is envisaged that such structures will form *in vivo*, although this is yet to be demonstrated.

We have used gel electrophoresis to examine the DNA alkylation and crosslinking properties of activated monocrotaline. We were able to determine the sequence-selective reaction of DHM in the major groove of DNA. In addition, we also detected the presence of a heat- and alkali-stable multiply crosslinked DNA structure with very low mobility in agarose and polyacrylamide gels. The presence of such multiple DNA crosslinks was further

*To whom correspondence should be addressed. Tel: +61 7 3274 9002; Fax: +61 7 3274 9003; Email: a.prakash@mailbox.uq.edu.au

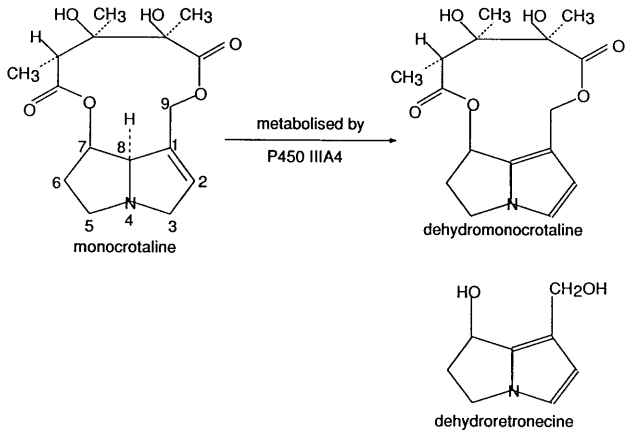

Figure 1. The chemical structure of monocrotaline and its metabolites, DHM and DHR.

confirmed using electron microscopy. Based on our observations, we present a scheme for the reaction of DNA with DHM that involves initial polymerization of the DHM monomer.

MATERIALS AND METHODS

Chemicals

All chemicals were purchased from Sigma unless otherwise noted. The toxicological effects of monocrotaline and DHM are not fully characterized. They are strong alkylating agents and should be handled carefully, preferably in a fume hood. Perspex and/or lead shields must be in place when handling uranyl acetate as well as the radioactive label [α-^{32}P]dATP and all DNA fragments labelled with it.

Preparation of DHM

Monocrotaline was converted to DHM by the method of Mattocks *et al.* (27), by dehydrogenation with *o*-chloranil(tetrachloro-1,2-benzoquinone). We confirmed the purity of the resulting pyrrole using NMR. It was stored at –80°C and, since it is highly unstable, it was made in small quantities as required.

DNA alkylation by DHM

DNA alkylation was carried out by the method of Prakash *et al.* (28). Briefly, a 375 bp *Eco*RI–*Bam*HI fragment of pBR322 (Promega) was 3′-end-labelled at the *Eco*RI site with [α-^{32}P]dATP (Bresatec, SA, Australia) with Klenow (Promega) and the fragment was isolated on a 4% non-denaturing polyacrylamide gel. Labelled DNA (at 10 000 c.p.m.) was incubated with 100 µM DHM at 37°C in 10 mM Tris–EDTA buffer (pH 7.6) and in 10 mM potassium phosphate buffer (pH 7.4) for various times (15, 30, 60 and 120 min). The reaction was stopped by precipitation in ethanol. The modified DNA was treated with 1 M piperidine at 90°C for 10 min. This causes cleavage of DNA at the alkylated N-7 of guanine residues (28). The solvent was removed by lyophilization before the samples were dissolved in a formamide dye. The samples and sequencing lanes corresponding to guanine and purine were electrophoresed on a 6% denaturing polyacrylamide gel at 50°C until the xylene cyanol dye front had migrated 25 cm. The gel was dried and exposed to X-ray film which was then developed.

Crosslinking assay

This assay makes use of the fact that the crosslinked DNA renatures after denaturation and co-migrates with native double-stranded DNA under agarose gel electrophoretic conditions (28). Plasmid DNA (pBR322) linearized with *Eco*RI was 3′-end-labelled with Klenow and [α-^{32}P]dATP. Labelled DNA (at 10 000 c.p.m.) was incubated for 1 h at 37°C with DHM at various concentrations in a total volume of 50 µl in 10 mM Tris–EDTA buffer (pH 7.6). The samples and a DNA control were denatured by heating at 90°C for 3 min in 50 µl of denaturing dye (30% DMSO), then chilled on ice. A native DNA control sample was cooled on ice in 50 µl of non-denaturing dye (50% sucrose). The samples were then electrophoresed on a 2% agarose gel at 40 V for 16 h. The gel was dried and exposed to X-ray film which was then developed.

DMS footprinting assay

This assay, which is an extension of the assay used to determine DHM-induced alkylation, was carried out to probe the site of DHM-induced crosslinks. DMS methylates DNA at N7 guanines, making them susceptible to piperidine-induced cleavage. When DNA is reacted with DMS followed by hot piperidine, a Maxam–Gilbert-type guanine sequencing ladder is generated. In the event of a piperidine-resistant crosslink in the DNA, DMS/piperidine treatment should result in a discontinuity at that site (23). The bands were quantified using Kodak Digital Science 1D Image Analysis software.

A 35 bp *Eco*RI–*Hin*dIII fragment of pBR322 was 3′-end-labelled and isolated on a 12% non-denaturing polyacrylamide gel, as for the alkylation study described above. Two sets of labelled DNA (at 10 000 c.p.m.) were incubated with 250 or 750 µM DHM at 37°C in 10 mM Tris–EDTA buffer (pH 7.6) for various times (15, 30 and 60 min). The reaction was stopped by precipitating the DNA in ethanol. One set was treated with 1% DMS in the presence of calf thymus DNA, at room temperature for 1 h. The reaction was stopped by ethanol precipitation and the samples from both sets were then treated with 1 M piperidine at 90°C for 10 min. The solvent was removed by lyophilization before the samples were dissolved in a formamide dye. The samples and a sequencing lane corresponding to guanine were electrophoresed on a 20% denaturing polyacrylamide gel at 50°C until the xylene cyanol dye front had migrated 12 cm. The gel was dried and exposed to X-ray film which was then developed.

The sequence of the *Eco*RI–*Hin*dIII 35 bp fragment is:

5′-AA ^{1}TTCTCATGTT ^{11}TGACAGCTTA ^{21}TCATCGATAA ^{31}GCT

3′-TT AAGAGTACAA ACTGTCGAAT AGTAGCTATT CGA

The ^{32}P-labelled nucleotides are underlined. The numbers in superscript correspond to the assigned pBR322 nucleotide sequence numbers.

Electron microscopy

Plasmid pBR322 DNA was linearized with *Eco*RI. The enzyme was removed by phenol/chloroform/isoamyl alcohol (25:24:1) extraction and the DNA was precipitated with 5 M sodium chloride and ethanol. DNA was reacted with DHM at a 1:5 ratio of molar concentrations at 37°C for 60 min in 50 µl of 10 mM

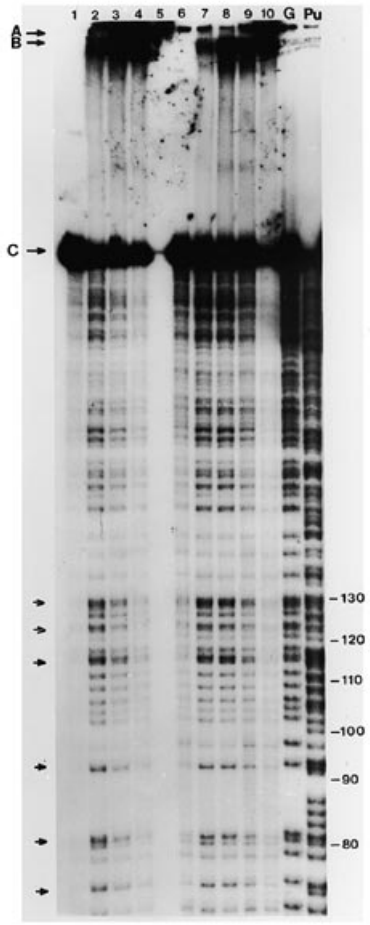

Figure 2. Autoradiogram of a 6% denaturing polyacrylamide gel showing the N7-G alkylation pattern of the ^{32}P-3′-end-labelled *Eco*RI–*Bam*HI fragment of pBR322 plasmid DNA exposed to 100 µM DHM for various lengths of time. Lanes 1–5, in 10 mM Tris–EDTA buffer (pH 7.6); lanes 6–10, in 10 mM potassium phosphate buffer (pH 7.4). Lanes 1 and 6, untreated control DNA; lanes 2 and 7, 15 min; lanes 3 and 8, 30 min; lanes 4 and 9, 60 min; lanes 5 and 10, 120 min. Lanes G and Pu correspond to guanine and purine sequence ladders. The numbers on the right side correspond to the base positions in the fragment. Small arrows correspond to GG and GA sequences. Large arrows: A, IFC; B, ISC; C, unmodified DNA.

Tris–EDTA buffer (pH 7.6). A control sample of DNA without DHM was included. The hyperphase consisted of 25 µl of 2 M ammonium acetate, 4 mM EDTA (pH 7.5), 25 µl of cytochrome c at 0.4 mg/ml and 50 µl of the test sample solution. The hypophase was 0.25 M ammonium acetate (pH 7.5). The hyperphase was spread as described by Coggins *et al.* (29) and was adsorbed onto collodion-coated carbon grids, stained with 50 mM uranyl acetate (Probing and Structure, Queensland, Australia), 50 mM HCl and rotary shadowed with platinum/carbon. The grids were examined with an electron microscope operating at 80 kV.

RESULTS

Sequence selectivity of DHM-induced DNA adducts

Figure 2 shows an autoradiogram of the strand cleavage pattern produced by DHM-treated DNA. DHM induces piperidine-labile

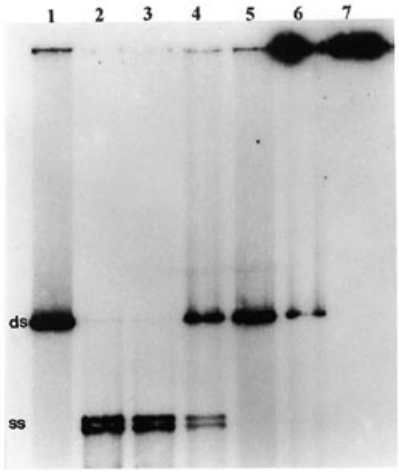

Figure 3. Agarose gel electrophoresis of linearized pBR322 plasmid DNA exposed to varying concentrations of DHM for 60 min then heat denatured at 90°C. Lane 1, untreated undenatured control DNA; lane 2, untreated denatured control DNA; lane 3, 1 µM DHM; lane 4, 10 µM DHM, lane 5, 100 µM DHM; lane 6, 1 mM DHM; lane 7, 10 mM DHM.

N7-G alkylation with a moderate preference for 5′-G in GG and GA sequences (Fig. 2, small arrows; bases 80–81, 115–116, 123–124 and 129–131 are 5′-GG, bases 74 and 93 are 5′-GA). In comparison, G residues at base numbers 70, 78, 97, 138, 144 and 151 show much weaker band intensities (since the bands in the upper half of the gel run much closer to each other than those in the bottom half, we labelled only the bottom half for clarity). The reaction is optimal in 10 mM TE buffer (lanes 1–5). A similar trend is seen in 10 mM potassium phosphate buffer (lanes 6–10), indicating that it is not due to drug–Tris complex formation as reported for chloroethylnitrosoureas (30). The band intensity reached a maximum within the first 15 min (lane 2), which is the first time point, and decreases with time (lanes 3–5). Lower time points were not attempted. The intensities of the bands (arrow C) corresponding to the unmodified DNA in DHM-treated samples (lanes 3–5) do not recover to control level (lane 1). Instead, piperidine-resistant bands of lower mobility are seen just below the wells (arrow B, probably a DNA interstrand crosslink, ISC) and in the wells (arrow A, multiply crosslinked DNA or an interfragment crosslink, IFC). The reduction in the band intensity of piperidine-labile DNA with the concomitant increase with time in the intensity of piperidine-resistant bands at the top of the gel indicates the formation of a super DNA structure, which provided protection to N7-alkylated guanines from piperidine.

DNA crosslinking assay

An autoradiogram of the agarose gel electrophoretic pattern of DHM-induced crosslinked DNA is shown in Figure 3. Crosslinking is DHM concentration-dependent (lanes 3–7) and is complete by 100 µM concentration. In addition to ISC, which co-migrates with the native DNA control (lanes 4–6), the figure shows bands trapped in the wells at concentrations >100 µM (lanes 6 and 7) and is nearly complete at 1 mM concentration (lane 6). Intermediate concentrations are not shown in this gel. The presence of this band, which corresponds to a large DNA

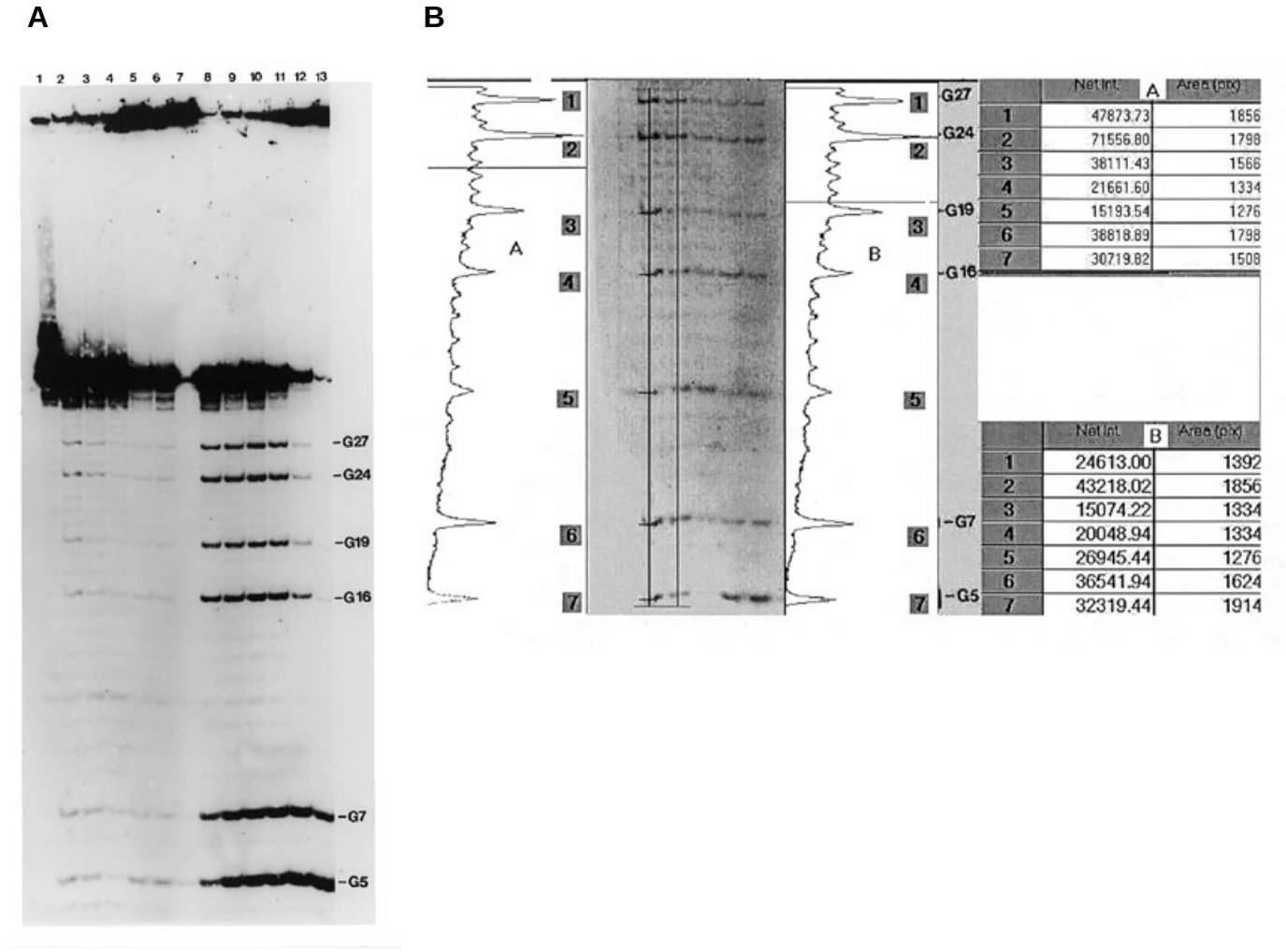

Figure 4. DMS crosslink footprinting assay. (**A**) Autoradiogram of a 20% denaturing polyacrylamide gel showing piperidine-induced strand cleavage pattern in the ^{32}P-3′-end-labelled *Eco*RI–*Hin*dIII fragment of pBR322 plasmid DNA. Lanes 1–7, DHM-treated DNA samples subjected to hot piperidine; lanes 8–13, DNA samples treated with DMS followed by hot piperidine. Lane 1, untreated control DNA; lanes 2–4 and 9–11, 250 μM DHM; lanes 5–7 and 12–13, 750 μM DHM; lanes 2, 5, 9 and 12, 15 min; lanes 3, 6, 10 and 13, 30 min; lanes 4, 7, and 11, 60 min; lane 8 corresponds to a G (guanine) sequencing reaction. (**B**) Densitometric scans and analyses of lanes 2 (marked A) and 3 (marked B) from the gel in (A).

fragment that fails to enter the gel at the given electrophoresis conditions, is indicative of the formation of IFC.

DMS footprinting assay

Figure 4 shows the results from the DMS assay. The first seven lanes correspond to alkylation kinetics studies similar to that shown in Figure 2, the main difference being the fragment lengths (375 versus 35 bp). When the DHM-treated DNA was subjected to piperidine, the 250 μM DHM samples (lanes 2–4) produced band patterns similar to the guanine sequencing lane (lane 8). There are no 5′-GG sequences in this fragment but there are four GA sequences (G5, G7, G24 and G27), one GT (G16) and one GC (G19) sequence. Please note that these numbers are different from the pBR322 sequence numbers shown in the earlier section. The preference for GA sequences is not visually obvious but densitometric analysis (Fig. 4B) clearly indicates that the intensities of G16 and G19 are at least 10–20% less than that of G24 and G27. Increasing the incubation time with DHM still yielded mainly piperidine-labile bands. However, in the 750 μM samples (lanes 5–7), bands resistant to piperidine were found in the wells even for the earliest time point (lane 5). The piperidine-labile bands got fainter with increasing incubation times and after 1 h incubation, all the radioactivity was found in the well (lane 7).

In order to detect the site of the DNA crosslink, we probed the above DHM-treated DNA with DMS. With the unmodified DNA fragment, DMS will methylate all guanines at the N7 site with near equal selectivity, which can then be subjected to piperidine-induced cleavage. This will generate a Maxam–Gilbert-type guanine sequencing ladder, as is observed in lane 8. However, in the event of a piperidine-resistant crosslink in the DNA, DMS/piperidine treatment should result in a discontinuity at that site because of the attachment of the piperidine-cleaved strand to a full-length strand in the case of ISC (23) or several full-length DNA fragments in the case of IFC.

When the DHM-treated DNA samples were probed with DMS, the 250 μM samples generated a guanine ladder (lanes 9–11)

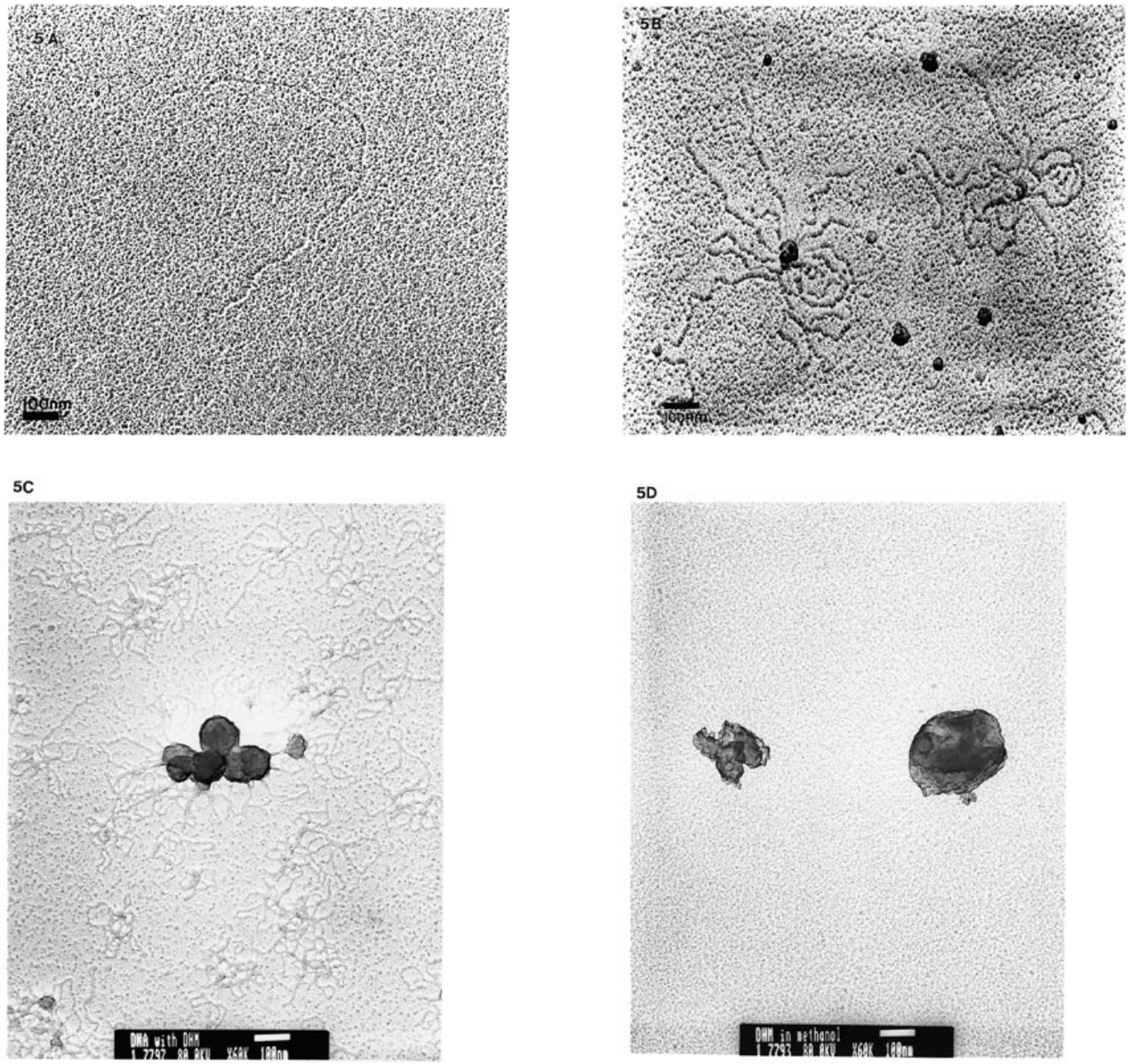

Figure 5. Electron micrographs of linearized pBR322 plasmid DNA. (**A**) Untreated control DNA; (**B** and **C**) DNA exposed to 1 mM DHM for 60 min; (**D**) 1 mM DHM in the absence of DNA.

similar to the sequence ladder. However, with 750 µM samples, there was an unambiguous discontinuity beyond the first two G bands (lanes 12 and 13). The bands corresponding to the unmodified DNA fragment fraction reduced in intensity while much of the high molecular weight product still remained in the wells.

Electron microscopy

Figure 5A–C shows electron micrographs of linearized pBR322 plasmid DNA (Fig. 5A) and DHM-induced multiply crosslinked plasmid DNA (Fig. 5B and C). A similar result was obtained by Reed *et al.* (31) using DHR. The multiple crosslinks appear to be joined at a focal point, seen as a dark spot. Similar spots are also observed in Figure 5D, which is an electron micrograph of a sample of DHM in the absence of DNA.

DISCUSSION

Monocrotaline toxicity has been attributed to its reactivity with cellular DNA after heme-thiolated monooxygenase activation (15). The exact mechanism of toxicity is still unclear, although various workers have implicated DNA ISC and DNA–protein

crosslinks (19–21). There has been a significant variation between the toxicity of different pyrrolizidine alkaloids which moderately correlates with *in vitro* DNA crosslinking levels (19). We undertook this study to characterize the reaction of DHM with DNA.

We found that DHM alkylates N7 of guanines in the major groove of DNA, which has not been reported before. The reaction is rapid and there is a preference for guanines in 5′-GG and 5′-GA sequences (Fig. 2). In addition to these lesions, we also observed DNA bands of low mobility which appeared at a slower rate and seemed to reach a maximum by 1 h of incubation. These low mobility bands were observed with labelled DNA fragments of differing sizes (35, 375 and 4363 bp fragments in this work). Since DHM is a potential bifunctional alkylating agent, we suspected that these bands might represent highly crosslinked DNA fragments (IFC). Electron microscope work confirmed the formation of such crosslinked product (Fig. 5B and C). However, we were surprised to find that up to 12 pBR322 fragments (4363 bp long) were attached to each other at or near one point rather than forming a highly branched network, as one might have expected of a multiply crosslinked DNA. A similar DNA crosslinked structure has been reported for DHR (31). Such multiple crosslinks have not been observed for other crosslinking agents. One trivial explanation for the formation of this highly polymerized structure is a DHM-induced DNA aggregation similar to that observed with heavy metal cations (32). However, such aggregated DNA will have a more branched appearance and aggregation is reversible upon addition of EDTA or heat. These structures, apart from having a radial appearance, are heat- and piperidine-resistant and are not reversible by any other chemical treatment. A more probable mechanism is the initial polymerization by DHM (26). Instead of forming a branched polymer, DHM could in fact form a dendrimer-like structure (33) since it contains two electrophilic (C7 and C9) sites and one nucleophilic site. Therefore, one might expect that an electrophilic site on one molecule could react with the nucleophilic site (C2=C3 double bond) of another. It is more likely that the C7 site is more often involved than C9, as it is more electrophilic than C9. This may progress in such a way as to form a spherical structure with mostly the intact C9 alkylating arms of the surface-bound DHM molecules sticking out radially. These weak electrophilic sites may then have the potential to react with many fragments of DNA at N2 of guanines to form the observed piperidine- and heat-resistant DNA super structures. It is important to point out that in a similar case, the strong electrophilic centre on MMC, a DHM analogue, reacts with N7 guanine in the major groove while the weaker electrophilic centre mainly reacts with N2 guanine in the minor groove (23; below). Figure 6 depicts this in a diagrammatic form. Cationic polyamidoamines form similar polymers, called Starburst dendrimers, which are used as a vehicle to carry DNA fragments for efficient transfection into cultured cells (33). The electron microscope work (Fig. 5D) confirmed the formation of a DHM polymer. Evidence of the existence of IFC was also provided by DNA crosslink studies, in which DHM preincubated in buffer prior to the addition of DNA led to more extensive DNA IFC and reduced ISC (data not shown). The fact that we observed near complete formation of IFC structures at 1 mM concentration using a full-length pBR322 fragment (Fig. 3, lane 6) suggests that it may have biological importance. In comparison, chloroethylnitrosoureas form only a small percentage of ISC at this concentration under the same conditions (34,35). Further, DNA crosslinks in Madin Darby bovine kidney epithelial cells required DHM concentrations in the range 300–500 μM (21). Lee and Gibson, working with U-77,779, a bifunctional analogue of CC1065, noted that an *in vitro* crosslinking assay such as ours requires concentrations of any bifunctional agent several orders of magnitude (~10^4 times for 4.4×10^3 bp pBR322) greater than that required in cell culture studies in which chromosomal DNA (4.4×10^7 bp) is involved (36).

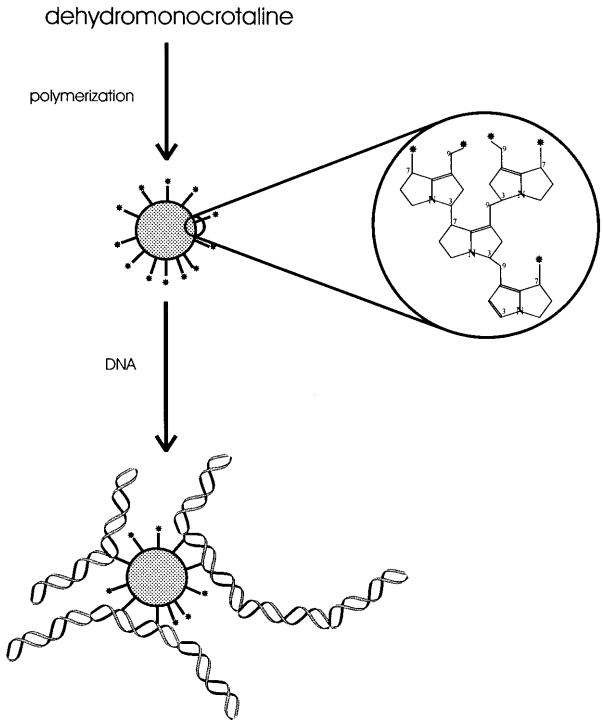

Figure 6. Schematic representation of the polymerization of DHM and reaction of the polymer with DNA.

Based on our results, we know that these lesions do not involve N7 of guanine but may occur via the exocyclic amino group of guanine in the minor groove of DNA (16). Such minor groove crosslinks are known to be heat- and piperidine-resistant (23). The factors governing the alkylation preferences of N7 and N2 of guanine are not well understood. Pearson's theory of electrophile–nucleophile interactions based on hard and soft acid–base (HSAB) predicts that a strong electrophile (C7 in our case) will preferentially react with a strong nucleophile such as N7-G, whereas a weak electrophile (C9 in our case) would prefer a weak nucleophile such as N2-G (37).

MMC is an antibiotic with chemotherapeutic properties and has a structure similar to that of PAs. When it is enzymatically or chemically activated, MMC alkylates DNA in the major groove at the N7 position of G at 5′-GG-3′ and 5′-GTC-3′ sequences (23). It also produces piperidine-resistant lesions which subsequently lead to ISC at 5′-CG-3′ sequences. Tomasz *et al.* (24) have shown by NMR that this crosslink occurs in the minor groove at the N2 of guanine. Weidner *et al.* (38), who investigated the sequence preference of crosslinks induced by DHM and MMC using hydroxy radical footprinting, also found that 5′-CG sites were the preferred site of crosslinking for this class of compounds. In order to determine the site of crosslinking for DHM, we used a 35 bp fragment containing a CG sequence (at G18–19) as well as AG

and TG sites, which are clearly not appropriate for crosslinking. Our findings show that DMS produces a discontinuity after the second G at the 3′ end. This G is not an ideal ISC site since the closest G on the opposite strand is at least three bases away and, based on molecular modeling studies (38), crosslinking at this site is unlikely due to distance constraints. A more likely suggestion for the discontinuity is a non-sequence-specific crosslink via N2-G alkylation of different fragments leading to IFC.

It is interesting to note that the intensities of piperidine-labile bands diminish with a concomitant increase in the intensities of the piperidine-resistant bands as incubation time is increased (Figs 2 and 4). The possibility that N7 guanine alkylation is reversible with time can be ruled out because of the lack of a corresponding increase in intensity of the bands of unmodified DNA. It is more likely that the formation of DNA IFC leads to steric protection of the labile N7-G sites from alkali (piperidine) or alkylating agents (DMS). This was confirmed by the DMS assay, in which only the two guanines closest to the labelled end were accessible to DMS attack in the IFC lanes while the middle guanines were protected from DMS (Fig. 4). The guanines close to the unlabelled 5′ end were also likely to be sensitive to DMS attack, but they will not show up in the gel.

While our results show that steric factors provide protection of alkylated N7-G sites from further chemical attack, it is unlikely that they will be able to provide direct protection from heat, which leads to depurination; however, once depurinated, they will be able to shield these sites from strand breakage, which requires alkali. Thus, the possibility that N7-G sites may take part in IFC can be discounted, because the heat treatment would lead to depurination and subsequent reversal of crosslinking. On the other hand, IFC through N2-G will be able to shield N7-G sites from strand breakage (but not depurination) in the presence of heat and alkali, thus explaining the stability of these structures to such treatments.

In this study, we have shown that DHM can modify DNA in several different ways *in vitro*. It is possible that all of them may contribute to DHM-mediated DNA damage *in vivo* and, if so, not all of them will be repaired in the same manner. DNA lesions in the major groove are believed to be repaired by base excision repair involving glycosylases, whereas minor groove lesions are repaired by nucleotide excision repair. Recently, Braithwaite *et al.* (39) have shown that DNA lesions induced by polycyclic aromatic hydrocarbons (PAHs) are repaired by both pathways, the contribution from each pathway depending on the extent of depurination from N7-G sites induced by the particular PAH in question. Crosslinks are thought to be the hardest to repair, usually involving DNA recombination. In the case of DHM polymer-induced IFC, repair will be even more difficult because of the potential steric hindrance to repair enzymes from binding to DNA. Apart from DNA, the DHM polymer may also be able to react with proteins in a similar fashion. Future studies will address the possibility of polymer formation in cells and its relevance to PA toxicity.

ACKNOWLEDGEMENTS

We thank Dr Bronwyn Cribb (Centre for Electron Microscopy and Microanalysis, University of Queensland) for assisting us with experimental design of the electron microscopy study. The NRCET is funded by the National Health and Medical Research Council, Queensland Health, The University of Queensland and Griffith University.

REFERENCES

1 Bras,G., Jelliffe,D.B. and Stuart,K.L. (1954) *Am. Med. Assoc. Arch. Pathol.*, **57**, 285–300.
2 Mohabbat,O., Younos,M.S., Merzad,A.A., Srivastava,R.N., Sediq,G.G. and Aram,G.N. (1976) *Lancet*, **2**, 269–271.
3 Tandon,B.N., Tandon,H.D., Tandon,R.K., Narendranathan,M. and Joshi,Y.K. (1976) *Lancet*, **2**, 271–272.
4 Kumana,C.R., Ng,M., Lin,H.J., Ko,W., Wu,P.C. and Todd,D. (1985) *Gut*, **26**, 10–104.
5 Sperl,W., Stuppner,H., Gassner,I., Judmaier,W., Dietze,O. and Vogel,W. (1995) *Eur. J. Pediat.*, **154**, 112–116.
6 Hooper,P.T. and Scanlan,W.A. (1977) *Aust. Vet. J.*, **53**, 109–114.
7 McEwan,T. (1979) *Aust. Vet. J.*, **55**, 601–602.
8 Johnson,A.E. and Molyneux,R.J. (1984) *Am. J. Vet. Res.*, **45**, 26–31.
9 Gaul,K.L., Gallagher,P.F., Reyes,D., Stasi,S. and Edgar,J. (1994) In Colegate,S.M. and Dorling,P.R. (eds), *Plant Associated Toxins*. CAB International, Wallingford, UK, Chapter 26, pp. 137–142.
10 Svoboda,D.J. and Reddy,J.K. (1972) *Cancer. Res.*, **32**, 908–913.
11 Hooson,J., Grasso,P. and Mattocks,A.R. (1973) *J. Pathol.*, **110**, 8–9.
12 Peterson,J.E., Jago,M.V., Reddy,J.K. and Jarrett,R.G. (1983) *J. Natl Cancer Inst.*, **70**, 381–386.
13 Hirono,I., Ueno,I., Yamaji,T. and Haga,M. (1983) *Cancer Lett.*, **20**, 191–198.
14 Chan,P.C., Mahler,J., Bucher,J.R., Travlos,G.S. and Reid,J.B. (1994) *Toxicon*, **32**, 891–908.
15 Miranda,C.L., Reed,R.L., Guengerich,F.P. and Buhler,D.R. (1991) *Carcinogenesis*, **12**, 515–519.
16 Robertson,K.A. (1982) *Cancer Res.*, **42**, 8–14.
17 Petry,T.W., Bowden,G.T., Huxtable,R.J. and Sipes,I.G. (1984) *Cancer Res.*, **44**, 1505–1509.
18 Robertson,K.A., Seymour,J.L., Hsia,M.T. and Allen,J.R. (1977) *Cancer Res.*, **37**, 3141–3144.
19 Hincks,J.R., Kim,H.Y., Segall,H.J., Molyneux,R.J., Stermitz,F.R. and Coulombe,R.A.,Jr (1991) *Toxicol. Appl. Pharmacol.*, **111**, 90–98.
20 Wagner,J.G., Petry,T.W. and Roth,R.A. (1993) *Am. J. Physiol.*, **264**, L517–L522.
21 Kim,H.Y., Stermitz,F.R. and Coulombe,R.A.,Jr (1995) *Carcinogenesis*, **16**, 2691–2697.
22 Mattocks,A.R. and Legg,R.F. (1980) *Chem. Biol. Interact.*, **30**, 325.
23 Prakash,A.S., Beall,H., Ross,D. and Gibson,N.W. (1993) *Biochemistry*, **32**, 5518–5525.
24 Tomasz,M., Lipman,R., Chowdary,D., Pawlak-Verdine,G.L. and Nakanishi,K. (1987) *Science*, **235**, 1204–1208.
25 Seawright,A.A., Hrdlicka,J., Wright,J.D., Kerr,D.R., Mattocks,A.R. and Jukes,R. (1991) *Vet. Hum. Toxicol.*, **33**, 286–287.
26 Mattocks,A.R. (1978) In Keeler,R.F., Van Kampen,K.R. and James,L.F. (eds), *Effects of Poisonous Plants on Livestock*. Academic Press, New York, NY, pp. 177–187.
27 Mattocks,A.R., Jukes,R. and Brown,J. (1989) *Toxicon*, **27**, 561–567.
28 Prakash,A.S., Denny,W.A., Gourdie,T.A., Valu,K.K., Woodgate,P.D. and Wakelin,L.P. (1990) *Biochemistry*, **29**, 9799–9807.
29 Coggins,L.W. (1987) In Sommerville,J. and Scheer,U. (eds), *Electron Microscopy in Molecular Biology*. IRL Press, Oxford, UK, pp. 1–29.
30 Chen,F.-X., Bodell,W.J., Liang,G. and Gold,B. (1996) *Chem. Res. Toxicol.*, **9**, 208–214.
31 Reed,R.L., Ahern,K.G., Pearson,G.D. and Buhler,D.R. (1988) *Carcinogenesis*, **9**, 1355–1361.
32 Duguid,J.G. and Bloomfield,V.A. (1995) *Biophys. J.*, **69**, 2642–2648.
33 Kukowska-Latallo,J.F., Bielinska,A.U., Johnson,J., Spindler,R., Tomalia,D.A. and Baker,J.R. (1996) *Proc. Natl Acad. Sci. USA*, **93**, 4897–4902.
34 Prakash,A.S. and Gibson,N.W. (1992) *Carcinogenesis*, **13**, 425–431.
35 Hayes,M.T., Bartley,J., Parsons,P.G. and Prakash,A.S. (1997) *Biochemistry*, **36**, 10646–10654.
36 Lee,C.-S. and Gibson,N.W. (1991) *Cancer Res.*, **51**, 6586–6591.
37 Carlson,R.M. (1990) *Environ. Health Perspect.*, **87**, 227–232.
38 Weidner,M.F., Sigurdsson,S.T. and Hopkins,P.B. (1990) *Biochemistry*, **29**, 9225–9233.
39 Braithwaite,E., Wu,X. and Wang,Z. (1998) *Carcinogenesis*, **19**, 1239–1246.